

# Spectroscopy of buffer-gas cooled vanadium monoxide in a magnetic trapping field

Jonathan D. Weinstein, Robert deCarvalho, Karine Amar, Andreea Boca, Brian C. Odom, Bretislav Friedrich,<sup>a)</sup> and John M. Doyle

*Department of Physics, Harvard University, Cambridge, Massachusetts 02138*

(Received 16 March 1998; accepted 14 May 1998)

Spectroscopy of buffer-gas cooled vanadium monoxide (VO) is performed in the presence of a magnetic trapping field and at low field. VO is created via laser ablation. A helium buffer gas, chilled by a dilution refrigerator, cools  $10^{12}$  VO molecules to  $1.8 \pm 0.2$  K within 10 ms. The measured rotational temperature is  $1.5 \pm 0.8$  K. Spatially resolved Zeeman spectra allow the magnetic broadening terms of several optical transitions to be determined. The density of VO decays with a characteristic time of 60 ms, thus precluding the observation of trapping. © 1998 American Institute of Physics. [S0021-9606(98)01831-5]

## INTRODUCTION

In several experiments over the past decade, evaporative cooling has been employed on magnetically trapped atoms to produce a variety of cold, dense atomic gases. Ultracold atoms produced in this manner have been used to push forward high-precision spectroscopy and to produce Bose condensates.<sup>1,2</sup> In general, magnetic trapping and evaporative cooling should be applicable to any paramagnetic species. However, until recently, experiments have been limited to the alkalis, which can be loaded optically, and atomic hydrogen. The loading of hydrogen into a magnetic trap relied on the (unique) low binding energy of atomic hydrogen to a superfluid helium surface. This special surface was used to thermalize the hydrogen atoms to temperatures below the depth of the magnetic trap.<sup>3</sup> The magnetic trapping of alkalis has relied on precooling in a magneto-optical trap.<sup>4</sup> Most of the alkalis (cesium, lithium, rubidium, and sodium) have been magnetically trapped. Although optical cooling methods work well for the alkalis, applying the same to molecules is extremely problematic. The primary difficulty is the repeated closed-cycle scattering of photons necessary for efficient cooling. While alkali atoms have simple closed cycles conveniently located in the visible wavelength range, molecules' complex level structure prohibits such simple cycling. A method using multiple frequencies to excite many transitions has been recently proposed.<sup>5</sup> So far, no neutral molecule has been trapped, by any means.

Buffer-gas loading was proposed as a method to trap any paramagnetic species, atom or molecule.<sup>6</sup> Recently, we trapped atomic chromium and europium using buffer-gas loading.<sup>7,8</sup> In those experiments, the atoms thermalized with cold helium gas. High numbers of trapped atoms ( $\sim 10^{12}$ ) and high densities ( $\sim 10^{12}$  cm<sup>-3</sup>) were attained.

We report here experiments with buffer-gas cooled vanadium monoxide (VO) in a magnetic trapping field. We did not observe trapping. The rapid loss of VO that prevented the

observation of trapping is discussed in detail below. We were, however, able to do extensive spectroscopy on the cold VO gas. The principles of buffer-gas loading are described in detail in a previous paper.<sup>6</sup> We give a brief description below, using a molecule as the example species. A magnetic trap is formed by a set of current-carrying coils that produce a magnetic field minimum in free space. The trapping region is filled with helium buffer gas maintained at cryogenic temperatures ( $\leq 1$  K). The (hot) molecules are introduced into the trap where they diffuse through the helium gas and thermalize via elastic collisions. Molecules in weak-field seeking magnetic states are contained by the magnetic trapping fields. As the molecules are thermally distributed, they can evaporate from the trap and stick to the cell walls that surround the trapping region. The rate of evaporation is determined by  $\eta$ , the ratio of the trap depth to the temperature of the molecules. For a sufficiently large  $\eta$ , this evaporation is slow enough that a large fraction of the molecules may be held for a long time. This time can be made sufficiently long that the helium gas can be (cryo-)pumped out of the trapping region without appreciable loss of the trapped molecules. Because this technique relies only on elastic collisions with the buffer gas and on the magnetic state of the species, it should be applicable to any magnetic species which can be cleanly introduced into the cryogenic environment.

## EXPERIMENT

The experimental apparatus used in our work with VO is described in earlier publications.<sup>8,9</sup> A short description is given here. The production, thermalization, and trapping of VO all take place within a copper cell. This cell is attached to a dilution refrigerator which cools the cell to temperatures of 0.05 to 1.5 K. The cell is placed inside a quadrupole magnetic field generated by a set of superconducting coils in the anti-Helmholtz configuration. The magnetic coils are contained by a titanium cask, and the entire assembly is immersed in liquid helium at 4.2 K. The cell is filled with <sup>3</sup>He gas ( $\sim 10^{17}$  cm<sup>-3</sup>). This serves as the buffer gas. The molecules are produced within the cell by laser ablation of a

<sup>a)</sup>Also at Department of Chemistry, Harvard University, Cambridge, Massachusetts 02138.

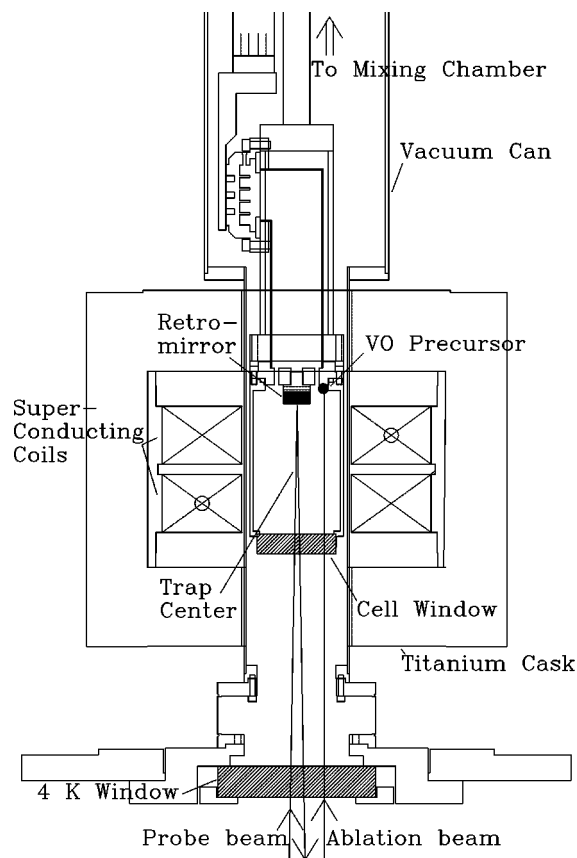


FIG. 1. Diagram of the experimental apparatus. The superconducting magnet is immersed in liquid helium. Optical access to room temperature is provided by a set of borosilicate windows at the cell temperature, 4, 77, and 300 K. Only the 4 K window is shown in the figure. The 77 and 300 K windows lie directly below the 4 K window. The YAG beam and the probe beam enter through the same set of windows.

solid precursor. To permit optical access for the ablation laser and the probe beam, a window is mounted on the bottom of the cell. A mirror is placed on the top interior surface of the cell to reflect the probe beam back out of the apparatus. See Fig. 1.

We chose vanadium monoxide as our candidate molecule for a variety of reasons. VO has been of previous interest to spectroscopists because of its presence in the atmospheres of cool red stars.<sup>10</sup> Studies of VO in solid matrices have also been performed.<sup>11,12</sup> It is of particular spectroscopic interest because Zeeman spectroscopy has not been performed on gas phase VO. In fact, no study of a gas phase  $^4\Sigma$  state in a strong magnetic field has been performed.<sup>13</sup> VO's strong transition around 574 nm (easily accessible with a dye laser) allows us to optically detect the VO.<sup>14</sup> The zero-field spectrum of VO has already been studied and analyzed.<sup>15</sup> In addition, a large Franck-Condon factor and large vibrational spacing allow efficient detection via frequency-resolved fluorescence.<sup>16</sup> Finally, the  $X^4\Sigma^-$  lowest energy rotational states of VO are paramagnetic, with magnetic moments of  $\sim 1-3$  Bohr magneton ( $\mu_B$ ). It should be noted that a highly magnetic state such as  $^4\Sigma$  is not necessary for trapping; our work with atoms indicates that species with one Bohr magneton magnetic moment or greater can be trapped in our apparatus.<sup>7</sup>

VO molecules are produced by laser ablation of a solid sample of specially prepared  $V_2O_5$ . The ablation pulse used has  $\sim 20$  mJ total energy, 4 ns pulse width, and is at a wavelength of 532 nm (frequency doubled Nd:YAG). In our initial work with production of VO, it was found that if  $V_2O_5$  powder was simply compacted into a solid plug, considerable dust was produced in ablation. A preparation technique was developed for the  $V_2O_5$  that greatly reduced this effect. No visible dust was seen during the ablation of the specially prepared precursor. A fine  $V_2O_5$  powder<sup>17</sup> is compressed into a 3 mm diameter copper tube with a pressure of  $\sim 10^5$  psi. It is then baked in air at a temperature of about 600 °C for about 1 min. The resulting material looks somewhat dull and black. During the development of this process, we also successfully ablated other precursors and detected two other monoxide molecules: specially prepared  $Ho_2O_3$  to produce holmium monoxide (HoO) and specially prepared  $NbO_2$  to yield niobium monoxide (NbO). VO gave the largest absorption in these initial room-temperature experiments. For this reason (and others) we pursued low-temperature work primarily with VO.

VO is detected through laser absorption or laser-induced fluorescence spectroscopy by exciting the  $C^4\Sigma^- \leftarrow X^4\Sigma(0,0)$  transition at 574 nm.<sup>15</sup> In the case of fluorescence spectroscopy, the light from the decay to the  $\nu=1$  electronic ground state is detected.<sup>16</sup> Fluorescence was more sensitive than absorption, which was limited by vibrations of the cryogenic apparatus. For fluorescence detection, a colored glass filter and a bandpass interference filter were used to block light from the scattered probe beam, as well as light from the ablation process (the ablation "glow").<sup>18</sup> Fluorescence spectroscopy was performed with a photomultiplier tube (PMT), and, separately, with an intensified charge coupled device (CCD) camera. The PMT was used in the lock-in detection of fluorescence induced by an acousto-optically modulated beam. The performance of this detection was limited by fluorescing epoxy glue present in our cell.<sup>19</sup> We were able to obtain a sensitivity of optical density  $10^{-5}$  (on the relevant time scales) providing us with observations of VO densities spanning six orders of magnitude. Densities as low as  $10^5$  cm<sup>-3</sup> were detectable. Fluorescence spectroscopy done with the camera provided images of the (frequency-resolved) fluorescence from the trap region. This will be discussed in detail below. The timing of the experiment is controlled by a computer, as is the data acquisition. All times cited in this paper are given in reference to the single molecule-creating ablation pulse at  $t=0$ .

Absorption spectroscopy avoids complications due to the ablation glow. Also, using absorption spectroscopy makes it straightforward to determine the optical density of the atom cloud, and hence the total number of VO molecules present in the cell. Early-time ( $\leq 10$  ms) absorption spectra are shown in Fig. 2. In our spectra, the absorption at a given frequency and time was obtained by setting the frequency of the laser, ablating the VO, measuring the absorption as a function of time, and averaging the absorption over the appropriate time window. Spectra were obtained by repeating this process at different probe frequencies. The ablation process is sufficiently consistent shot-to-shot that meaningful

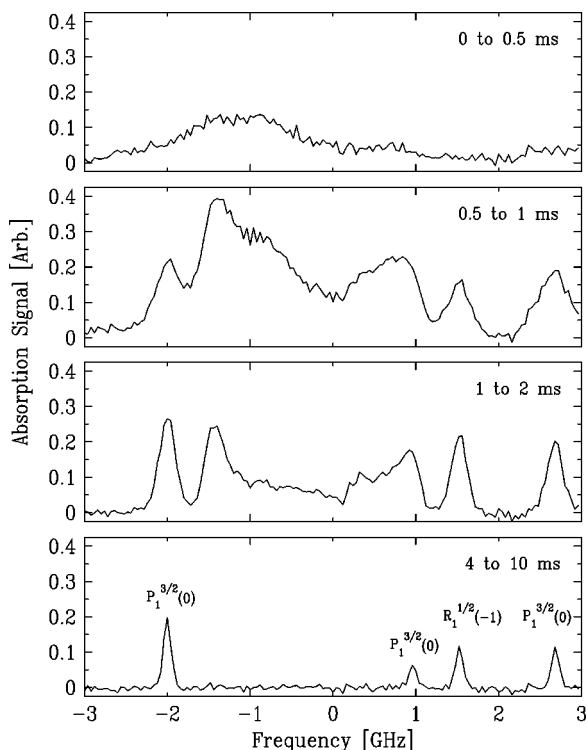


FIG. 2. Early-time absorption spectra of VO, with the trap off. The line-width narrows over time due to thermalization (and cooling) of VO via collisions with the helium buffer gas. Final spectra consist of identified VO lines, but earlier spectra show the presence of species other than VO ( $X^4\Sigma^-, \nu=0$ ).

spectra can be taken in this manner. At 10 ms, the spectra can be clearly identified as VO. However, the signal observed at earlier times ( $<4$  ms) cannot be entirely reconciled with the known VO lines in this spectral region. Lines which are not VO ( $X^4\Sigma^-, \nu=0$ ) are present. This probably indicates that other molecular species or excited states of VO are formed and destroyed over this short time period.

While the lines in this spectral region are all identifiable as VO ( $X^4\Sigma^-, \nu=0$ ) for times  $\geq 10$  ms, this is not the case in all spectral regions. Unidentified lines of intensity one-tenth that of the strongest VO lines were found around  $17,423\text{ cm}^{-1}$ . The source of these spectral features was not determined. However, they are not due to any known line of atomic vanadium, atomic or molecular oxygen, or VO ( $X^4\Sigma^-, \nu=0$ ).

The spectral lines of VO can be observed to rapidly narrow as the VO cools in the buffer gas. See Fig. 2. Assuming that the width of the transition is due to Doppler broadening, the translational temperature of the VO molecules can be obtained. The VO cools to a temperature of  $1.8 \pm 0.2$  K for times  $t > 10$  ms. This temperature is somewhat higher than the temperature of the cell prior to ablation, 0.3 K. However, this does not mean that the VO is out of thermal equilibrium with the buffer gas and cell walls. Using resistance thermometry, the cell temperature is observed to rise due to heating by the ablation pulse. Although this thermometry is not responsive on millisecond time scales, a temperature rise to about 1 K is seen on a 1 s time scale. Thus, the measured VO translational temperature is roughly equal to the cell tem-

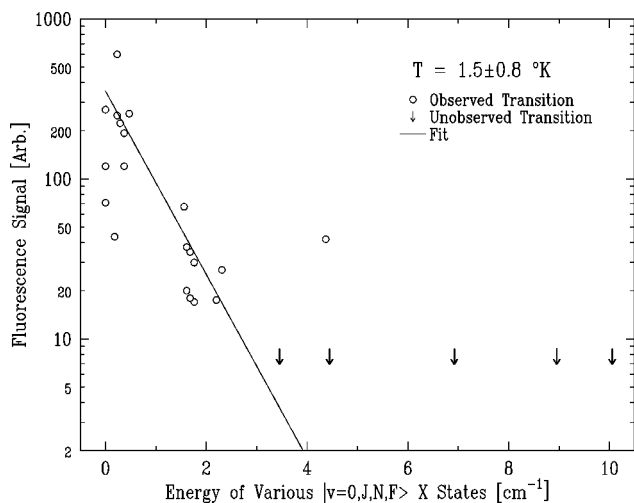


FIG. 3. Fluorescence signal versus the energy of the state from which the given transition originates. Fluorescence signal normalized for level degeneracy. Data taken with magnet off. Arrows denote VO transitions which are not observed. The fit is to a Boltzmann distribution and indicates a temperature of  $1.5 \pm 0.8$  K.

perature. Based on these measurements, it is very likely that the translational temperature of the VO has come into thermal equilibrium with the buffer gas.

The rotational temperature of the VO is also determined. This is done through analysis of the relative strength of the VO hyperfine/rotational spectral lines. The various lines of VO, and the energies of the ground electronic rotational and hyperfine states from which they originate, have been previously identified.<sup>15</sup> From the relative fluorescence signal of these identified lines, the relative populations of the originating states can be identified. (It is assumed that the observed transitions have identical oscillator strengths.) We integrated the fluorescence signal over a 3–23 ms time window.<sup>20</sup> Fitting a temperature to the populations of these states gives  $T_{\text{rot}} = 1.5 \pm 0.8$  K. See Fig. 3. This can be compared to the measured translational temperature of  $1.8 \pm 0.2$  K. We conclude that translational/rotational equilibrium is reached on a time scale of  $\leq 10$  ms. This indicates a He–VO translational and rotational relaxation cross section of  $\geq 10^{-16}\text{ cm}^2$ .

Using our absorption spectra and the published radiative lifetime of the  $C^4\Sigma^-, \nu=0$  state ( $73 \pm 2\ \mu\text{s}$ <sup>14</sup>), we have also determined the total number of VO molecules produced. A single ablation pulse ( $\sim 20$  mJ) produces  $10^{12}$  molecules at 1.8 K. This implies a density of  $10^{10}$ . About 80% of the VO molecules are in the two closely spaced lowest rotational states ( $N=1, J=0.5$ ) and ( $N=0, J=1.5$ ). Using an acousto-optic modulator to chop the probe beam, we were able to measure the lifetime of the  $C^4\Sigma^-, \nu=0$  state in the trap environment as  $\sim 10^{-7}$  s.

The temporal behavior of the VO molecule was investigated by observing the frequency-resolved fluorescence while continuously exciting particular transitions. A time profile with the magnetic trapping fields off is shown in Fig. 4. This time profile is quite different than those observed for atomic europium and chromium produced under similar conditions.<sup>8,7</sup> The “knee” in the time profile is qualitatively different than the smoother, roughly exponential, time pro-

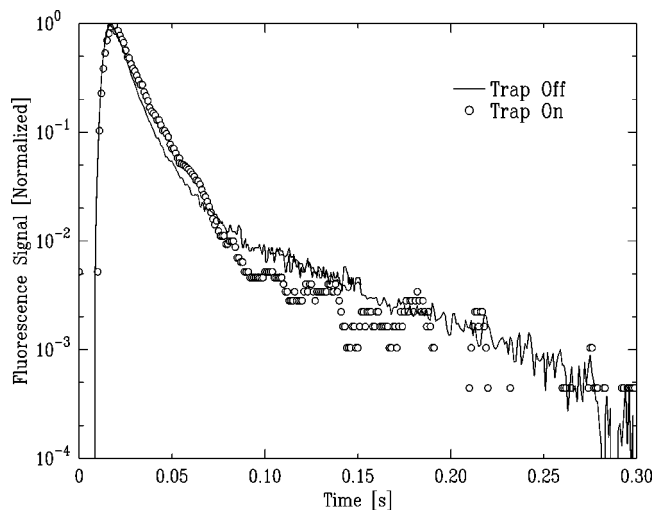


FIG. 4. Time profile of VO, with the trapping fields off, and with the trap on. The VO is detected on the  $P_1^{3/2}(0)$  transition. This time behavior is typical for all observed VO transitions.

files for Eu and Cr. In addition, the rate of decay of the VO is more rapid than that seen for atoms produced under similar conditions: Eu and Cr decay with an exponential time constant of roughly 250 ms (in the absence of magnetic fields), while the VO time constant is  $\sim 60$  ms for times  $100 < t < 300$  ms. Both of these differences suggest that the disappearance of the VO molecules is caused by a different mechanism than with the atomic species. In the case of the atomic species, the temporal behavior was consistent with loss due to diffusion to the walls, where the atoms stick and are lost.

## DISCUSSION

While we have not been able to conclusively identify the mechanism responsible for the VO loss, some conclusions can be drawn. It is unlikely that the dominant mechanism behind the VO decay is diffusion to the walls of the cell. The diffusion time constant for VO would be roughly comparable to that observed for atomic species, and the shape of the decay would also be similar. We verified that the loss was not primarily diffusion by varying the density of buffer gas by up to an order of magnitude with little change in the loss rate of VO. In addition, it is unlikely that the VO is disappearing primarily through two-body interactions between VO molecules. Although the decay of the VO does slow somewhat over time, it does not slow as much as would be expected if it were due to VO–VO processes. By modifying the probe beam power and duty cycle, we found the disappearance of the VO signal was not due to optical pumping effects. One plausible mechanism for the loss of VO is chemical reactions with other species (molecules, clusters, or dust) produced by the laser ablation.

This model of reactive loss finds some support in our observations of the ablation-induced afterglow. This glow was observed with or without the presence of the probe beam. In our measurements, the VO signal can be distinguished from this glow spectroscopically and with other techniques that vary depending on our detection method. It is

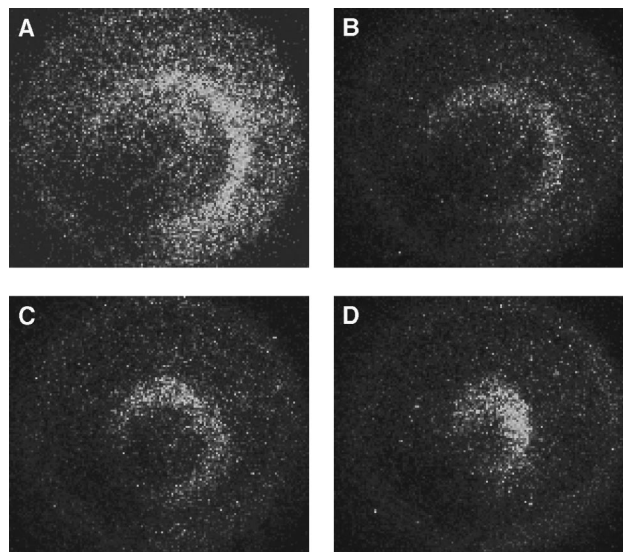


FIG. 5. Images of VO in the magnetic trap. The images are of frequency-resolved fluorescence from the  $P_1^{3/2}(0)$  transition (integrated from 1 to 5 ms) and were taken with a CCD camera. The magnetic trap has a depth of 2.3 T and an average radial gradient of 1.0 T/cm. Successive pictures are taken at different frequencies, with a spacing of 0.1 GHz.

interesting to note that the decay in the magnitude of this glow has a temporal behavior similar to the laser-induced fluorescence signal. It may be that the glow originates (in part) from photon emission following chemical reactions within the trapping region. This would be consistent with the presence of reactive species that cause the decay of the VO population.

We attempted to magnetically trap the VO, typically using trap depths of 1.5–2.3 Tesla (corresponding to radial field gradients of 0.7–1.0 T/cm). However, in the presence of the trapping fields, the peculiar decay rate of VO remained the same. See Fig. 4. Shown are data from a specific high-field transition [one of the narrow hyperfine peaks of the  $P_1^{3/2}(0)$  transition, see below]. These data are characteristic of all VO signals seen in the trap at high field. This unmodified disappearance of VO would be consistent with the above hypothesis describing the decay. In general, the trap would slow the rate at which the low-field seeking states of VO stick to the walls. However, because the dominant decay mechanism is not diffusion out of the trap, the presence of the trapping potential has a negligible effect on the disappearance of the VO.

With the magnetic trapping field on, the VO spectrum changes dramatically from its comparably well understood zero-field counterpart. The spatially varying magnetic field results in inhomogeneous broadening of the VO transitions. The inhomogeneous magnetic broadening, can, to a large extent, be directly reduced to the underlying magnetic shift as a function of field. We observed this by using an intensified CCD camera to spatially resolve VO molecules at different magnetic fields. Because of the geometry of our experiment, the fluorescence from atoms at a given field strength (and hence frequency shift) will appear as a ring when imaged by our camera. See Fig. 5. The signal from different transitions can be resolved and identified, and their

TABLE I. Zeeman spectroscopy of various transitions at high field.

Transition	$\Delta\mu(\mu_B)$	Ring spacing (GHz)
$P_1^{3/2}(0)$	$-0.07 \pm 0.02$	$1.41 \pm 0.05$
$R_1^{1/2}(-1)$	$-0.16 \pm 0.03$	$1.46 \pm 0.05$
$R_1^{3/2}(0)$	$+0.02 \pm 0.01$	$0.70 \pm 0.05$

frequency shift as a function of magnetic field can be determined.

## CONCLUSION

We have attempted to theoretically calculate the magnetic shifts of the VO ground and excited states, based on previously obtained zero-field molecular parameters<sup>15</sup> and the Hamiltonian of Ref. 21. The differences in the magnetic moments of ground/excited state pairs (which we label as  $\Delta\mu$ ) for various transitions were obtained from these calculations. However, our calculations were unreconcilable with the magnetic shifts obtained from the observed spectra.

Experimentally, we found that each observed  $|J''S''N''\rangle \leftarrow |J'S'N'\rangle$  transition consists of a set of eight narrowly broadened peaks, in addition to a wide ( $\sim 1 \text{ cm}^{-1}$ ) background on both sides of the narrow structure. We attribute the “narrow” structure to transitions between Zeeman levels with well matched magnetic moments. These transitions are split into eight peaks by the high-field hyperfine structure of VO. The broad structure surrounding these hyperfine peaks is attributed to the same electronic transitions as the peaks they surround, but between Zeeman levels with poorly matched magnetic moments. This broad structure is magnetically broadened to such an extent that the individual hyperfine peaks are no longer resolvable. Using the state notations of Ref. 15, Table I lists magnetic moment differences and line spacings observed for our narrow peaks in high field (0.3–2 Tesla).

The lack of a theory that accurately corresponds to our observations precludes identification of the specific Zeeman levels from which our narrow peaks originate. Thus, we cannot tell whether we are monitoring the behavior of strong-field seeking or weak-field seeking states. We would like to determine the relative populations of the strong-field and weak-field seeking states because it would be interesting to determine the rate at which the molecules thermalize into the strong-field seeking states through collisions with the helium buffer gas and with each other. (The strong-field seeking states are the lower energy states in a magnetic field.) Successful magnetic trapping relies on a sufficiently low rate of Zeeman state thermalization. Without a complete understanding of the Zeeman structure of VO, our analysis is tentative. However, the spectrally broad features (which appear on both sides of each spectrally narrow set) are quite suggestive about the relative populations of the various Zeeman states.

We assigned the narrow spectral features to  $\Delta m = 0$  transitions between the  $X^4\Sigma^-$  and  $C^4\Sigma^-(0,0)$  states, and, thus, the broad spectral features at lower (redshifted) and higher (blueshifted) frequencies would be due to  $\Delta m = -1$  and  $\Delta m = +1$  transitions, respectively. The  $P_1^{3/2}(0)$  line can only

have  $\Delta m = -1$  transitions from weak-field seeking states. Correspondingly, its  $\Delta m = +1$  transitions originate purely from strong-field seeking states. Thus, one can compare the behavior of the strong-field seeking and weak-field seeking states of VO by monitoring the behavior of the broad sidebands of the  $P_1^{3/2}(0)$  transition.

Such analysis is potentially complicated by the overlap of the broad sidebands of the  $P_1^{3/2}(0)$  transition with those of a transition without such restrictions on which states can undergo  $\Delta m = \pm 1$  transitions. Fortunately, this interfering transition is noticeably weaker, so that it should not significantly affect our analysis.

We were able to measure the time dependence of the broad peaks for  $\sim 100$  msec after the ablation. No significant difference could be seen between the time behavior of the blueshifted broad peak and that of the redshifted broad peak. If our interpretation of the broad structure is correct, then this would indicate that if the Zeeman states thermalize to the translational temperature, it is on a time scale  $\geq 100$  msec. However, our inability to definitively identify any broad transition as purely strong-field or weak-field seeking makes our interpretation inconclusive.

In conclusion, spectroscopy of VO has been performed at  $\sim 1$  K at low field and in the presence of a magnetic trapping field. The VO was produced via laser ablation of a solid vanadium oxide precursor. Cooling was accomplished with a helium buffer gas maintained at low temperatures by a dilution refrigerator. Rapid, field independent, depletion of VO was observed. It is surmised that this loss is due to chemical reactions of the VO with other species created during the ablation process. Camera-based spectroscopy of VO in the magnetic trapping field revealed Zeeman-induced spatial structure. Analysis of these spectra resulted in a determination of magnetic moment differences between ground and excited states associated with particular transitions. These observations are inconsistent with our calculations based on measured zero-field constants and the Hamiltonian of Ref. 21. The hyperfine splitting of VO was measured in high field. Some evidence found suggests the ratio of He–VO elastic to spin-relaxation cross sections is much greater than 10. We are hopeful that the VO loss mechanism observed in this experiment is not universal, but can be avoided using a “cleaner” production method. It may also be possible that the loss mechanism is unique to VO (or a class of molecules like VO) and laser ablation can be used to successfully produce other molecules for buffer-gas loading of magnetic traps.

## ACKNOWLEDGMENTS

This material is based upon work supported by the National Science Foundation under Grant No. PHY-9511951. One of us (J.D.W.) is supported by a National Science Foundation Graduate Research Fellowship.

<sup>1</sup>C. L. Cesar, D. G. Fried, T. C. Killian, A. D. Polcyn, J. C. Sandberg, I. A. Yu, T. J. Greytak, D. Kleppner, and J. M. Doyle, *Phys. Rev. Lett.* **77**, 255 (1996).

<sup>2</sup>M. H. Anderson, J. R. Ensher, M. R. Matthews, C. E. Wieman, and E. A. Cornell, *Science* **269**, 198 (1995); K. B. Davis, M. O. Mewes, M. R. Andrew, N. J. Vandrunen, D. S. Durfee, D. M. Kurn, and W. Ketterle,

- Phys. Rev. Lett. **75**, 3969 (1995); C. C. Bradley, C. A. Sackett, and R. G. Hulet, *ibid.* **78**, 985 (1997); see also, C. C. Bradley, C. A. Sackett, J. J. Tollett, and R. G. Hulet, *ibid.* **75**, 1687 (1995).
- <sup>3</sup>H. F. Hess, G. P. Kochanski, J. M. Doyle, N. Masuhara, D. Kleppner, and T. J. Greytak, Phys. Rev. Lett. **59**, 672 (1987).
- <sup>4</sup>E. A. Cornell, C. Monroe, and C. E. Wieman, Phys. Rev. Lett. **67**, 18 (1991).
- <sup>5</sup>J. T. Bahns, W. C. Stwalley, and P. L. Gould, J. Chem. Phys. **104**, 9689 (1996).
- <sup>6</sup>J. M. Doyle, B. Friedrich, J. Kim, and D. Patterson, Phys. Rev. A **52**, R2515 (1995).
- <sup>7</sup>J. D. Weinstein, R. deCarvalho, J. Kim, D. Patterson, B. Friedrich, and J. M. Doyle, Phys. Rev. A **57**, R3173 (1998).
- <sup>8</sup>J. H. Kim, B. Friedrich, D. P. Katz, D. Patterson, J. D. Weinstein, R. deCarvalho, and J. M. Doyle, Phys. Rev. Lett. **78**, 3665 (1997).
- <sup>9</sup>J. Kim, Ph.D. thesis, Harvard University, 1997 (unpublished).
- <sup>10</sup>H. Spinrad and R. F. Wing, Annu. Rev. Astron. Astrophys. **7**, 249 (1969).
- <sup>11</sup>P. H. Kasai, J. Chem. Phys. **49**, 4979 (1968).
- <sup>12</sup>L. B. Knight, Jr., R. Babb, M. Ray, T. J. Banisaukas, L. Russon, R. S. Dailey, and E. R. Davidson, J. Chem. Phys. **105**, 10237 (1996).
- <sup>13</sup>A. J. Merer, private communication.
- <sup>14</sup>L. Karlsson, B. Lindgren, C. Lundevall, and U. Sassenberg, J. Mol. Spectrosc. **181**, 274 (1997).
- <sup>15</sup>A. S.-C. Cheung, R. C. Hansen, and A. J. Merer, J. Mol. Spectrosc. **91**, 165 (1982).
- <sup>16</sup>F. S. Ortenberg and V. B. Glasko, Sov. Astron. **6**, 714 (1963); S. N. Suchard, in *Spectroscopic Data Vol. 1, Heteronuclear Diatomic Molecules* (IFI/Plenum, New York, 1975).
- <sup>17</sup>Aldrich Chemical. V<sub>2</sub>O<sub>5</sub> powder, 99.99%.
- <sup>18</sup>Schott glass OG 590 colored glass filter. Three-cavity interference band-pass filter, 10 nm full width at half maximum (FWHM), 610 nm center wavelength.
- <sup>19</sup>Stycast 1266 Clear, Grace Specialty Polymers.
- <sup>20</sup>Three data points had integration windows from 1–11 ms. These data were normalized for comparison to the 3–23 ms window data points.
- <sup>21</sup>M. Mizushima, in *The Theory of Rotating Diatomic Molecules* (Wiley, New York, 1975).